Molecular reorientations in liquid crystals pentyloxybenzylidine hexylanilene (PBHA) and butyloxybenzylidine octylanilene (BBOA)

S. Mitra,[1,*] K. Venu,[2] I. Tsukushi,[3] S. Ikeda,[4] and R. Mukhopadhyay[1,†]
[1]*Solid State Physics Division, Bhabha Atomic Research Centre, Mumbai 400 085, India*
[2]*School of Physics, University of Hyderabad, Hyderabad 500 046, India*
[3]*Department of Physics, Chiba Institute of Technology, 2-1-1, Shibazano, Chiba 275-0023, Japan*
[4]*Neutron Science Laboratory, Institute of Materials Structure Science, High Energy Accelerator Research Organization, Tsukuba, Ibaraki 305-0801, Japan*
(Received 16 January 2004; published 9 June 2004)

Molecular reorientational motions in undeuterated pentyloxybenzylidine hexylanilene (PBHA or 5O.6) and butyloxybenzylidine octylanilene (BBOA or 4O.8) as studied by the quasielastic neutron scattering (QENS) technique in their different mesophases are reported. Models are built up in stages to account for the experimental elastic incoherent structure factor (EISF). It is found that there exist simultaneous reorientational motions of the chain group and the reorientational motions of the whole molecule around its molecular axis in the smectic-*G*, smectic-*B*, and smectic-*C* phases. In smectic-*A* and nematic phases, additional body axis fluctuations are found to exist in both 5O.6 and 4O.8 systems. The average amplitude of body axis fluctuations is found to be ~15° and 25°, respectively, in the smectic-*A* and nematic phases of 5O.6, and ~14° and 29°, respectively, in 4O.8.

DOI: 10.1103/PhysRevE.69.061709 PACS number(s): 42.70.Df, 61.30.−v, 61.30.Cz, 78.70.Nx

I. INTRODUCTION

Liquid crystals usually exhibit several mesophases differing by the degree of ordering of the molecules and the dynamics of these molecules is influenced by the transition from one phase to the other. Molecules undergo several kinds of motions leading to complicated trajectories of protons in molecular fluids. Internal molecular vibrations, translational and rotational diffusion, etc., are such possible motions. Neutron scattering techniques are very suitable for studing these dynamics for its matching time scales and also protons having a large neutron scattering cross section make the experiments much easier. The difficulty of the interpretation of neutron data is due to the fact that many different kinds of molecular motion are observed simultaneously and thus are superimposed with one another in the experimental data. In particular, it may include effects from the translation diffusion of the molecules and random rotational motion of the whole molecules and/or part of them. However, it is sometimes possible to separate the different types of motion by selecting different instrumental resolution or by selective deuteration. Nevertheless, in this paper, an attempt has been made to separate out the various rotational components in two undeuterated liquid crystals.

The compounds belonging to the *n*O.*m* (alkyloxy benzylidine alkylanilenes) homologous series of liquid crystal, where, *n* and *m* represent the number of carbons in the end chains on either sides of the molecules, attracted considerable interest as, apart from their wider ranging applications, it is easy to systematically vary the molecular structure of these systems by varying *n* and *m* and to study the effect of such variations on the physical properties of these liquid crystals [1,2]. Though the collective fluctuations that liquid crystal exhibits, belonging to *n*O.*m* series was studied earlier using the NMR technique [3–9], very little information could be obtained about the detailed reorientational components associated with the different parts of the molecules. The interest here is to study the faster molecular motions in the mesomorphic phases and the change involved, if any, on going from one mesophase to the other. We have studied earlier [10] the reorientational motions of the 4O.4 liquid crystal at its different mesomorphic phases through the quasielastic neutron scattering (QENS) technique. Earlier QENS studies on the dynamics of liquid crystals were mainly based on deuterated terephthalylidene-*bis*-butylanilene (TBBA) [11–15] and para azoxy anisole (PAA) [16,17].

We report here molecular motions in undeuterated pentyloxybenzylidine hexylanilene (PBHA or 5O.6) and butyloxybenzylidine octylanilene (BBOA or 4O.8) as studied by the quasielastic neutron scattering (QENS) technique. The mesomorphic behavior displayed by the 5O.6 liquid crystal is [2,18]

$$K \xrightarrow{308.2\ \mathrm{K}} S_G \xrightarrow{313.2\ \mathrm{K}} S_B \xrightarrow{324.3\ \mathrm{K}} S_C \xrightarrow{325.8\ \mathrm{K}} S_A \xrightarrow{334.2\ \mathrm{K}} N \xrightarrow{346\ \mathrm{K}} I$$

and 4O.8 has a phase sequence [2]

$$K \xrightarrow{306\ \mathrm{K}} S_B \xrightarrow{322\ \mathrm{K}} S_A \xrightarrow{337\ \mathrm{K}} N \xrightarrow{352\ \mathrm{K}} I$$

where *K* is crystalline, *S* is smectic, *N* is nematic, and *I* is isotropic.

*An author to whom correspondence can be sent. Email address: smitra@apsara.barc.ernet.in
†An author to whom correspondence can be sent. FAX: ++91-22-2550 5151. Email address: mukhop@apsara.barc.ernet.in

The interest here is to study the molecular motions in the various smectic and nematic (N) phase of 5O.6 and 4O.8 and the change involved, if any, on going from one mesophase to the other.

II. EXPERIMENTAL DETAILS

QENS experiments were carried out using a high resolution LAM80-ET spectrometer at KENS, KEK, Japan [19]. LAM80-ET is an inverted geometry time of flight spectrometer. The high resolution has been achieved by using an array of mica analyzers in backscattering geometry. The (006) reflection of the mica analyzer provides an energy resolution, $\Delta E = 17$ μeV, at a fixed final energy of 1.92 meV with a Q range 0.25–1.65 Å^{-1} and the (004) reflection provides $\Delta E = 6.5$ μeV at a fixed final energy of 0.85 meV with a Q range 0.17–1.1 Å^{-1}. Powder samples wrapped in an aluminum foil in the shape of a hollow cylinder were put inside in a standard cylindrical aluminum sample holder and placed in a variable temperature cryostat. All the measurements were carried out by keeping the sample in the transmission mode. The thickness of the sample was so chosen that the transmission is above 92% to minimize the multiple scattering effects. The raw data in time of flight was normalized with respect to monitor counts and converted to $S(Q,\omega)$ using standard programs available in KEK, Japan. QENS measurements were performed at five different temperatures for 5O.6: 310 K (S_G), 318 K (S_B), 325 K (S_C), 328 K (S_A), and 335 K (N), and three different temperatures for 4O.8: 297 K (crystalline), 328 K (smectic A), and at 343 K (nematic). The samples are obtained from Frinton Laboratories, USA and used without further purification. The purity of the sample was ascertained by verifying that the phase transition temperatures agree with the reported values.

III. RESULTS AND DISCUSSION

In a neutron scattering experiment the measured intensity is proportional to the double-differential cross section [20],

$$\frac{\partial^2\sigma}{\partial\omega\,\partial\Omega} \propto \frac{k}{k_0}[\sigma_{coh}S_{coh}(Q,\omega) + \sigma_{inc}S_{inc}(Q,\omega)], \qquad (1)$$

where $S(Q,\omega)$ is known as the scattering law and the subscripts "*coh*" and "*inc*" denote the coherent and incoherent components. $\mathbf{k}$ and $\mathbf{k}_0$ are the final and initial wave vectors and $Q=|\mathbf{k}-\mathbf{k}_0|$. The liquid crystalline systems contain many protons and they have large incoherent neutron scattering cross sections (80 barns compared to its coherent part of 1.7 barns; the total cross section for C atoms: 5.5 barns, 4.2 barns for O and 12.4 for N). Therefore, in a neutron scattering experiment from a protonated system the observed dynamics mainly correspond to the self-correlation function of the protons. Equation (1) can then be written as

$$\frac{\partial^2\sigma}{\partial\omega\,\partial\Omega} \propto \frac{k}{k_0}[\sigma_{inc}S_{inc}(\mathbf{Q},\omega)]. \qquad (2)$$

For quasielastic events (energy transfer $\leqslant$2 meV), the incoherent scattering law can be approximated as [21]

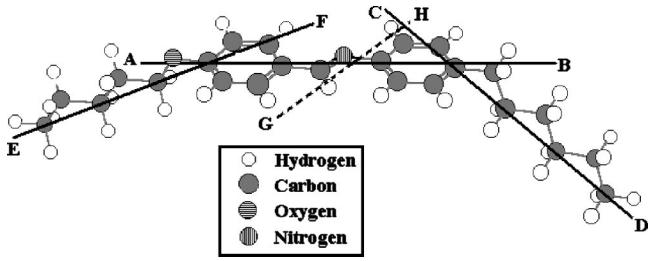

FIG. 1. Schematic of a 5O.6 liquid crystal and the different axis of rotation (see text).

$$S(Q,\omega) \propto A(Q)\delta(\omega) + [1 - A(Q)]L(\Gamma,\omega), \qquad (3)$$

where the first term is the elastic part and the second is the quasielastic one. $L(\Gamma,\omega)$ is a Lorentzian function

$$L(\Gamma,\omega) = \frac{1}{\pi}\frac{\Gamma}{\Gamma^2+\omega^2},$$

where Γ is the half width at half maximum (HWHM) of the Lorentzian function. It is convenient to analyze the data in terms of the elastic incoherent structure factor (EISF) which provides information about the geometry of the molecular motions. If $I_{el}(Q)$ and $I_{qe}(Q)$ are the elastic and quasielastic intensities, respectively, then the elastic incoherent structure factor (EISF) is defined as [20]

$$EISF = \frac{I_{el}(Q)}{I_{el}(Q) + I_{qe}(Q)}. \qquad (4)$$

Therefore, $A(Q)$ in Eq. (3) is nothing but the EISF. Analysis of the QENS spectra involves the determination of $A(Q)$ and Γ by a least square fit of Eq. (3) with the spectra after convoluting with the instrumental resolution.

A. Results of 5O.6

5O.6 is an elongated molecule containing two phenyl rings connected with a CH═N link (core group). Pentyloxy and hexyl chains are connected to the two phenyl rings at the end. The molecule is schematized in its *trans* conformation in Fig. 1. 5O.6 is more or less a balanced system, with five carbon atoms in one side and six carbon atoms on the other, an odd-even combination. The straight line passing through the centers of two phenyl rings can be defined as the molecular axis (line AB). For an elongated molecule like 5O.6, reorientation of the molecule is likely to occur around the molecular axis. The incoherent scattering law for a particle diffusing on a circle of radius a, with a diffusion coefficient D_r, for a powder sample, can be written as [22]

$$S_{inc}(Q,\omega) = A_0(Q)\delta(\omega) + \frac{2}{\pi}\sum_{l=1}^{\infty} A_l(Q)\frac{l^2D_r}{(l^2D_r)^2+\omega^2}, \qquad (5)$$

where the elastic and quasielastic structure factors are given by

$$A_0(Q) = \frac{1}{\pi}\int_0^{\pi} j_o(2Qa\,\sin x)dx, \qquad (6)$$

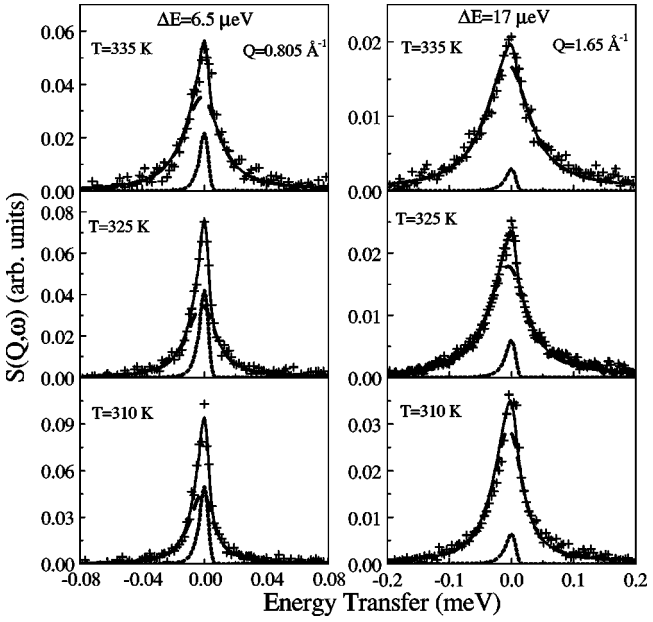

FIG. 2. Typical QENS spectra along with separated elastic (dotted) and quasielastic (dashed) components for a 5O.6 liquid crystal at different temperatures at $Q=0.805$ Å^{-1} and 1.65 Å^{-1}.

$$A_l(Q) = \frac{1}{\pi}\int_0^{\pi} j_o(2Qa\,\sin x)\cos(2lx)dx \quad (l = 1,2,\ldots,\infty). \tag{7}$$

Considering the molecule is rigid, i.e., side chains are bound to the core like a stick and having uniaxial rotational diffusion around the molecular axis, all the hydrogen atoms will have a different radius of rotation and Eqs. (6) and (7) should be averaged over the various distances of the hydrogen atoms to the rotation axis. Then the average elastic incoherent structure factor for a powder sample can be written as

$$\overline{A_0(Q)} = \frac{1}{N\pi}\sum_{i=1}^{N}\int_0^{\pi} j_o(2Qa_i\,\sin x)dx, \tag{8}$$

where N is the total number of hydrogen atoms in the molecule and a_i is the radius of rotation of the ith hydrogen atom.

QENS spectra for 5O.6 were separated into elastic and quasielastic parts as discussed above using Eq. (3) and the elastic incoherent structure factor (EISF) was determined. Separated elastic and quasielastic components along with typical QENS spectra are shown in Fig. 2 at $Q=0.805$ Å^{-1} and 1.65 Å^{-1} for different temperatures. Experimentally obtained EISF is shown in Fig. 3. It is quite evident from the figure that the experimental EISF for S_G,S_B,S_C phases are very close to each other suggesting similar geometry of the motion in these phases. However, the experimental EISF at S_A and nematic phases are considerably different. The theoretical EISF for uniaxial rotational diffusion around the molecular axis, as described by Eq. (8), is also shown in the same figure. Radii of rotation of different hydrogen atoms

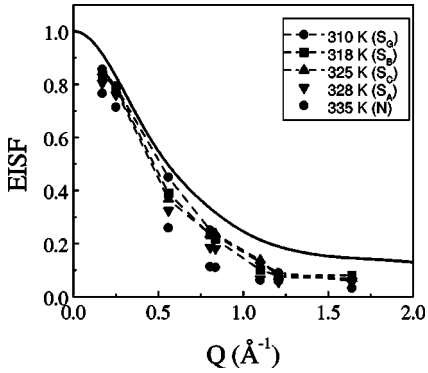

FIG. 3. Variations of experimental and theoretical EISF with Q for 5O.6. Theoretical EISF (solid line) is calculated by assuming only a uniaxial rotational diffusion of the whole molecule about the molecular axis.

are obtained assuming the structure of $n\mathrm{O}.m$ compounds given in Ref. [23]. It is evident that the rotation around the molecular axis alone could not explain the experimental EISF in any phase.

As found in other liquid crystal molecules (e.g., TBBA) [11], end chains can also reorient around its axis in addition to the rotation around the molecular axis. The hexyl and pentyloxy chain axes are shown by the line CD and EF, respectively, in Fig. 1. The EISF can also be obtained for a case where the molecule rotates around the molecular axis (*AB*) and the end chains rotate about the chain axis (*CD* and *EF*) simultaneously (as in a rigid molecule).

To calculate the EISF for simultaneous rotations in different segments of a molecule, one has to separately calculate the EISF for individual segments, namely hexyl chains, pentyloxy chains, and the core group of the molecule, and add the EISFs with a proper weighting according to the number of hydrogen atoms in each segment.

Let us consider first only the hexyl chain rotation. As the hexyl chain axis (*CD*) is at an angle of $\sim 30°$ with the molecular axis (*AB*) rotation of the whole molecule about the molecular axis, different hydrogen atoms in the hexyl chain follow different circular paths, depending on their distances from the *AB* axis. Further, due to the rotation of the chain about the chain axis, these hydrogen atoms will also undergo reorientational motions around the *CD* chain axis. Under the assumption that these two motions are uncorrelated, the total incoherent scattering functions can be written as the convolution of the two corresponding scattering laws described above. In that case, the corresponding total EISF for the hexyl chain hydrogen atoms can be written as the product of

$$A_{Hexyl}^{mol+chain}(Q) = A_{Hexyl}^{mol}(Q)A_{Hexyl}^{chain}(Q), \tag{9}$$

where $A_{Hexyl}^{mol}(Q)$ and $A_{Hexyl}^{chain}(Q)$ can be written using the uniaxial rotational diffusion model as described in Eq. (8),

$$A_{Hexyl}^{mol}(Q) = \frac{1}{N_{Hexyl}\pi}\sum_{i=1}^{N_{Hexyl}}\int_0^{\pi} j_o(2Qa_i\,\sin x)dx, \tag{10}$$

$$A_{Hexyl}^{chain}(Q) = \frac{1}{N_{Hexyl}\pi} \sum_{i=1}^{N_{Hexyl}} \int_0^{\pi} j_o(2Qb_i \sin x)dx. \quad (11)$$

Here N_{Hexyl} is the number of hydrogen atoms in the hexyl chains and a_i and b_i are the distances of various hydrogen atoms in the hexyl chain from the molecular (AB) axis and the chain (CD) axis, respectively.

Similarly, the EISF for the pentyloxy chain hydrogens can be obtained as

$$A_{Pentyl}^{mol+chain}(Q) = A_{Pentyl}^{mol}(Q)A_{Pentyl}^{chain}(Q). \quad (12)$$

Using the same methodology as discussed above, $A_{Pentyl}^{mol}(Q)$and $A_{Pentyl}^{chain}(Q)$ can be written as

$$A_{Pentyl}^{mol}(Q) = \frac{1}{N_{Pentyl}\pi} \sum_{i=1}^{N_{Pentyl}} \int_0^{\pi} j_o(2Qc_i \sin x)dx, \quad (13)$$

$$A_{Pentyl}^{chain}(Q) = \frac{1}{N_{Pentyl}\pi} \sum_{i=1}^{N_{Pentyl}} \int_0^{\pi} j_o(2Qd_i \sin x)dx. \quad (14)$$

Here, N_{Pentyl} is the number of hydrogen atoms in the pentyloxy chains and c_i and d_i are the distances of various hydrogen atoms in the pentyloxy chain from the molecular (AB) axis and the chain (EF) axis, respectively.

If the core group hydrogen atoms, belonging to the two phenyl rings and one hydrogen in the CH═N group, are undergoing only uniaxial rotational diffusion around the molecular axis, the corresponding EISF can be written as

$$A_{Core}(Q) = \frac{1}{N_{Core}\pi} \sum_{i=1}^{N_{Core}} \int_0^{\pi} j_o(2Qf_i \sin x)dx. \quad (15)$$

Here, N_{Core} is the number of core hydrogens and f_i's are the distances of various core hydrogens from the molecular (AB) axis.

Then, the total EISF for the whole molecule considering the reorientation of the whole molecule around the molecular axis (AB) and the reorientations of pentyloxy and hexyl chains around the pentyloxy (EF) and hexyl (CD) chain axes can be written as

$$A_{tot}^{mol+chain}(Q) = \frac{N_{Hexyl}}{N_{tot}} A_{Hexyl}^{mol+chain}(Q) + \frac{N_{Pentyl}}{N_{tot}} A_{Pentyl}^{mol+chain}(Q) + \frac{N_{Core}}{N_{tot}} A_{Core}(Q). \quad (16)$$

Here, $N_{tot}=N_{Hexyl}+N_{Pentyl}+N_{Core}$ is the total number hydrogens in the molecule.

The EISF calculated using Eq. (16) is shown in Fig. 4 along with the experimentally obtained EISF for S_G, S_B, and S_C phases. It is clear from Fig. 4 that the simultaneous rotation of the whole molecule around a long molecular axis and rotations of the end chains around the chain axis can very well explain the experimental EISF at S_G, S_B, and S_C phases. This indicates that, in addition to the whole molecule rotation around the long molecule axis, the end chain also rotates in the S_G,S_B,S_C phases. The variation of the HWHM of the quasielastic component with Q is shown in Fig. 5 for S_G, S_B, and S_C phases. It may be noted that the obtained HWHM is an average of the different motions contributed to the dynamics. However, the behavior of the HWHM with Q is consistent with the uniaxial rotational diffusion model [22]. Diffusion constants of both the rotation around the molecular axis and the rotation around the chain axis are difficult to separate out since the magnitude of the diffusion constant or the equivalent time scale for both motions are likely to be of the same order.

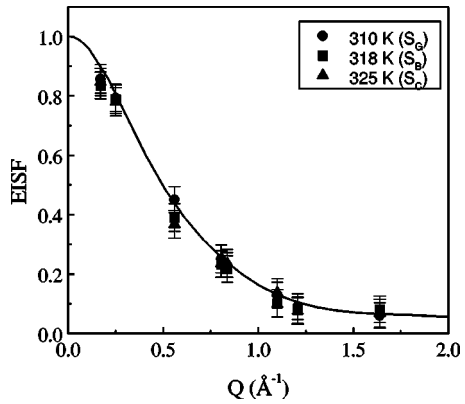

FIG. 4. Variations of experimental and theoretical EISF with Q for 5O.6. Theoretical EISF is calculated by assuming a uniaxial rotational diffusion of the whole molecule about the molecular axis and independent side chain rotations about the chain axis.

As can be seen in Fig. 3, it is evident that the EISF in S_A and nematic phases are considerably less than that of S_G,S_B, S_C phases at any particular Q value, suggesting further disorder than allowed by the simultaneous rotational diffusion along the long molecular axis and the end chain reorientations along the chain axis. The further disorder can come from the molecular body axis fluctuation about its equilibrium position in addition to the reorientation around the long molecular axis. However, the calculation of the scattering law considering all these motions is difficult since a description with a rate equation, as was done earlier, in such cases is not easy. Nevertheless, an expression of the EISF is available for such a case [12].

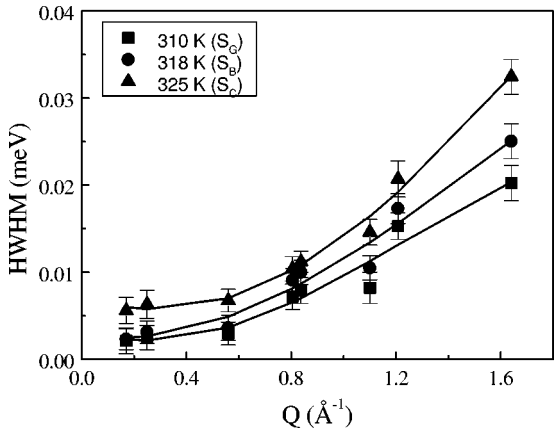

FIG. 5. Variation of the HWHM of the quasielastic component with Q in S_G, S_B, and S_C phases in 5O.6. Solid lines are guides to the eye.

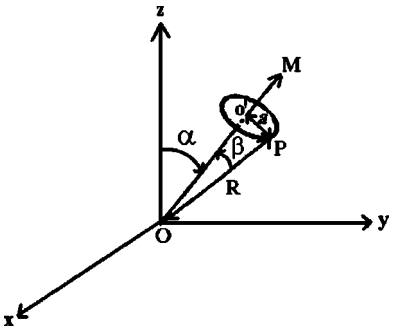

FIG. 6. Schematic figure of a particle P moving with respect to some laboratory frame (see text).

Consider an incoherent scattering center P moving around an axis OM on a circle of radius a centered on O' (Fig. 6). If β is the angle between OP and the axis OM and R is the distance of P from the origin, the fluctuations of the axis (OM) are described by the following normalized function as prescribed in Ref. [12]:

$$f(\alpha) = \frac{\delta}{2 \sinh \delta} \exp(\delta \cos \alpha), \tag{17}$$

where α is the angle between the instantaneous (OM) and the mean axis position (Oz) and δ is a parameter which characterizes the width of the angular distribution (peaked at $\alpha = 0$). The EISF in this case after powder averaging can be written as [12]

$$A_o(Q) = \sum_{l=0}^{\infty} (2l+1) j_l^2(QR) S_l^2(\delta) P_l^2(\cos \beta). \tag{18}$$

Also, $\sin \beta = a/R$ as evident from Fig. 6. S_l are the orientational order parameters which follow the recurrence relation

$$S_{l+1} = -\frac{2l+1}{\delta} S_l + S_{l-1} \tag{19}$$

with $S_0 = 1$ and $S_1 = \langle \cos \alpha \rangle = \coth \delta - (1/\delta)$.

The parameter $\Delta\alpha = \cos^{-1}(S_l)$ may be used to characterize the average amplitude of the oscillation. In Eq. (18), j_l and P_l are the spherical Bessel function and the Legendre polynomial of order l, respectively.

As shown in the reference, one recovers some limiting cases from Eq. (18). For example, if $\delta \to \infty$, Eq. (18) will be identical to Eq. (6), which is the EISF corresponding to the uniform uniaxial motion on the circle of radius a. Also in the case $\delta = 0$, one has $S_l = \delta_{l0}$ and Eq. (18) reduces to

$$A_0(Q) = j_0^2(QR), \tag{20}$$

which is nothing but the EISF for a powder sample corresponding to the isotropic rotation of a particle on a sphere of radius R. This means that by varying δ one can cover the entire domain between uniaxial to isotropic rotation.

The fluctuation of the long molecular axis occurs around the equilibrium position on the molecular axis. The most probable choice of the equilibrium position or the point of fluctuation is the projection of the center of mass of the whole molecule into the long molecular axis. The dashed line (GH) shows the fluctuating molecular axis in Fig. 1. The intersection of the dashed line with the molecular axis (AB) is the equilibrium position (the projection of the center of mass into the molecular axis) around which fluctuation can occur. Since the pentyloxy and the hexyl end chain rotations are likely to be present in addition to rotation and fluctuations of the molecular axis, one has to consider the motions of individual segments, namely hexyl chains, pentyloxy chains, and the core group of the molecule separately.

The EISF for the hexyl chain hydrogens, due to the rotation of the molecular axis and a fluctuation around its equilibrium position, can be expressed after averaging over the various distances of the hydrogens from the equilibrium point and the distances of the hydrogens from the molecular axis

$$A_{Hexyl}^{fluc+mol}(Q) = \frac{1}{N_{Hexyl}} \sum_{i=1}^{N_{Hexyl}} \sum_{l=0}^{\infty} (2l+1) j_l^2(Qp_i) S_l^2(\delta) P_l^2(\cos \beta_i) \tag{21}$$

and

$$\sin \beta_i = \frac{p_i}{q_i}. \tag{22}$$

Here q_i are the distances of hydrogen atoms in the hexyl chain from the point of fluctuation and p_i are the distances of the same hydrogen atoms from the molecular axis. Since the hydrogen atoms in the hexyl chain are also having rotations around the chain axis (CD), the total EISF for the hexyl chain, considering the fluctuation of the molecular axis, the rotation of hydrogen atoms around the molecular axis (AB), and the rotations of hydrogen atoms around the chain axis (CD) and assuming the two rotations are uncorrelated, can be written as

$$A_{Hexyl}^{fluc+mol+chain}(Q) = A_{Hexyl}^{fluc+mol}(Q) A_{Hexyl}^{chain}(Q), \tag{23}$$

where $A_{Hexyl}^{fluc+mol}(Q)$ and $A_{Hexyl}^{chain}(Q)$ are as described in Eqs. (21) and (11), respectively.

The EISF due to the fluctuations of the molecular axis and the rotation around the molecular axis can also be written in the same way for pentyloxy chain hydrogens, as described above. Therefore,

$$A_{Pentyl}^{fluc+mol}(Q) = \frac{1}{N_{Pentyl}} \sum_{i=1}^{N_{Pentyl}} \sum_{l=0}^{\infty} (2l+1) j_l^2(Qg_i) S_l^2(\delta) P_l^2(\cos \beta_i) \tag{24}$$

with $\sin \beta_i = g_i/h_i$. Here, g_i and h_i are the distances of pentyloxy chain hydrogens from the molecular axis and from the point of fluctuation, respectively. Considering the rotation of the pentyloxy chain around the chain axis (EF) in addition to the fluctuation and rotation of the molecular axis, total EISF for pentyloxy chain hydrogens can be written as

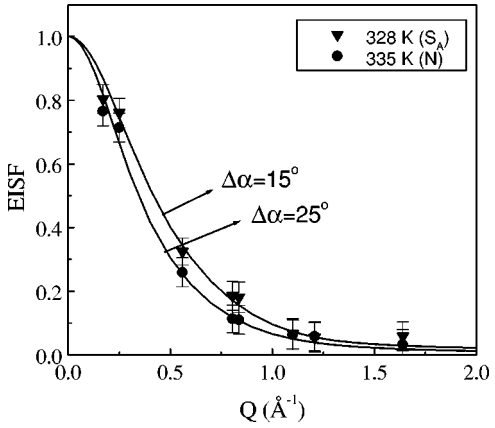

FIG. 7. Variations of experimental and theoretical EISF with Q for 5O.6. Theoretical EISFs (solid lines) are calculated by assuming a uniaxial rotational diffusion around the molecular axis plus side chain rotation plus body axis fluctuation.

$$A_{Pentyl}^{fluc+mol+chain}(Q) = A_{Pentyl}^{fluc+mol}(Q)A_{Pentyl}^{chain}(Q), \tag{25}$$

where $A_{Pentyl}^{fluc+mol}(Q)$ and $A_{Pentyl}^{chain}(Q)$ are as described in Eqs. (24) and (14), respectively.

Since the core group consisting of two phenyl rings and the CH═N group is only undergoing rotation around the molecular axis and the fluctuation of the molecular axis around the point of fluctuation, EISF can be written as

$$A_{Core}^{fluc+mol}(Q) = \frac{1}{N_{Core}} \sum_{i=1}^{N_{Core}} \sum_{l=0}^{\infty} (2l+1) j_l^2(Qt_i) S_l^2(\delta) P_l^2(\cos\ \beta_i) \tag{26}$$

with $\sin \beta_i = t_i/v_i$. Here t_i and v_i are the distances of core group hydrogen atoms from the molecular axis and from the point of fluctuation, respectively, and N_{Core} is the number of hydrogens in the core group.

Then, the total EISF for the whole molecule, considering the reorientation of the whole molecule around the molecular axis (AB), the fluctuation of the molecular axis, and the reorientations of pentyloxy and hexyl chains around pentyloxy (EF) and hexyl (CD) chain axes can be written as

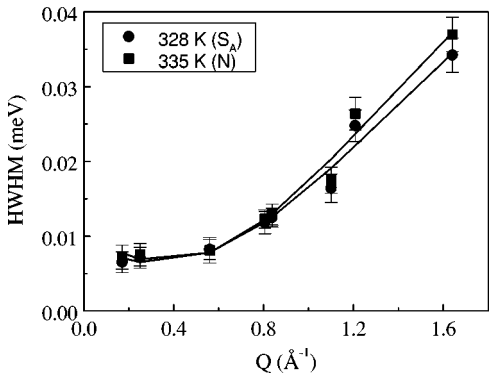

FIG. 8. Variation of the HWHM of the quasielastic component with Q in S_A and nematic phases in 5O.6. Solid lines are guides to the eye.

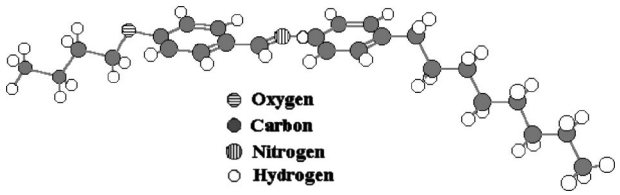

FIG. 9. Molecular conformation of the 4O.8 liquid crystal.

$$A_{tot}^{fluc+mol+chain}(Q) = \frac{N_{Hexyl}}{N_{tot}} A_{Hexyl}^{fluc+mol+chain}(Q) + \frac{N_{Pentyl}}{N_{tot}} A_{Pentyl}^{fluc+mol+chain}(Q) + \frac{N_{Core}}{N_{tot}} A_{Core}^{fluc+mol}(Q). \tag{27}$$

Here $N_{tot} = N_{Hexyl} + N_{Pentyl} + N_{Core}$ is the total number of hydrogens in the molecule.

To calculate the EISF according to Eq. (27), the distances of all the hydrogen atoms from the point of fluctuation, from the molecular axes, and the distances of end chain hydrogens from the respective chain axis are required. Then one can calculate the theoretical EISF for a given value of δ. It is to be noted that the infinite sum occurring in Eqs. (21), (24), and (26) over l cannot be truncated at a small l value in our experimental Q range due to the molecular dimension. In the summation terms up to at least $l=20$ were found necessary. Since for a given value of δ one can calculate the order parameter S_1 and eventually the average amplitude of fluctuation $\Delta\alpha[=\cos^{-1}(S_1)]$, one can calculate EISF curves for different values of $\Delta\alpha$. The EISF calculated with different values of $\Delta\alpha$ is shown in Fig. 7.

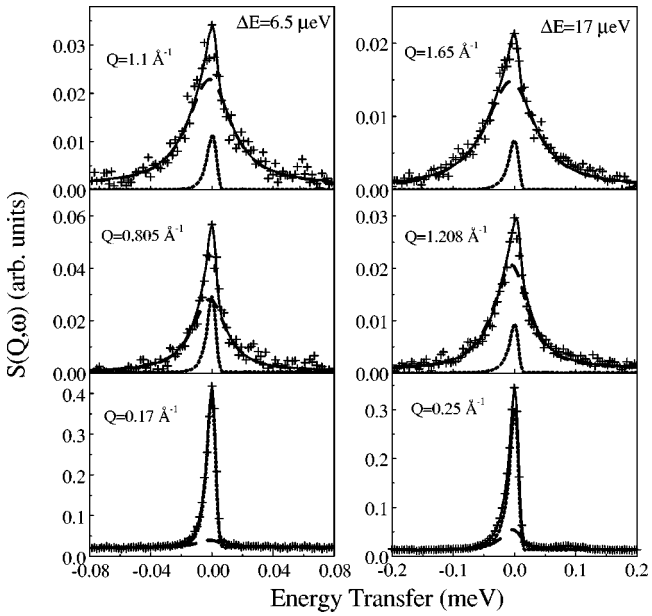

FIG. 10. Typical QENS spectra along with separated elastic (dotted) and quasielastic (dashed) components for the 4O.8 liquid crystal in the S_A phase at 328 K.

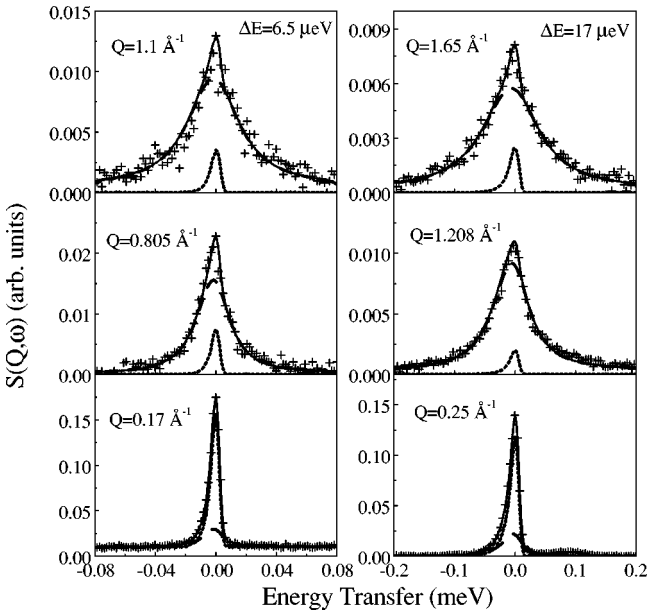

FIG. 11. Typical QENS spectra along with separated elastic (dotted) and quasielastic (dashed) components for the 4O.8 liquid crystal in the nematic phase at 343 K.

It can be seen that with $\Delta\alpha=15°$ and 25°, the calculated EISF can satisfactorily explain the experimental EISF at smectic *A* and nematic phases, respectively. So it can be said that, assuming the body of the molecule 5O.6 is rigid in its *trans* conformation, the whole molecular motion of 5O.6 can be described by the superposition of a uniaxial rotational diffusion around its long molecular axis, plus fluctuation of this axis around its equilibrium orientation in addition to the pentyloxy and hexyl chain reorientation around the chain axis. The fluctuation of the long molecular axis is characterized by an order parameter $S_1=\langle\cos(\Delta\alpha)\rangle=0.97$ in smectic *A* phases and 0.91 in nematic phases. The variation of the HWHM of the quasielastic component with *Q* is shown in Fig. 8 for S_A and *N* phases. Unfortunately, the determination of correlation times in both the phases is not possible at present, because the incoherent scattering law for this type of motion is not available. However, one can notice much less of a difference in the values of HWHM at particular *Q* values at both the phases, particularly at low *Q* values. One can, therefore, infer that the time scale of motions is very similar in smectic *A* and nematic phases. Slightly faster motion may be observed in the nematic phase compared to that of the smectic *A* phase.

B. Results of 4O.8

The same methodology is also applied for data analysis to the other member of the *n*O.*m* series, 4O.8. The molecule is schematized in its *trans* conformation in Fig. 9 as for the structure reported in Ref. [23]. 4O.8 is a less balanced system than the 5O.6 and, further more, it is an even-even type in terms of the number of carbon atoms in the side chains. Like the 5O.6 system this also shows a variety of mesophases as mentioned in Sec. I. Experiments were carried

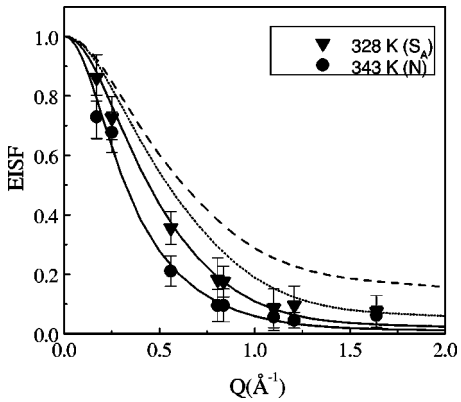

FIG. 12. Variations of experimental and theoretical EISF with *Q* for 4O.8. Theoretical EISF is calculated by assuming a uniaxial rotational diffusion of the whole molecule around the molecular axis plus side chain rotation plus body axis fluctuation.

out in its smectic *A* and nematic phases. Typical QENS spectra with the separated elastic and quasielastic components are shown in Figs. 10 and 11 in the S_A (at 328 K) and *N* phases (at 343 K), respectively. Figure 12 shows the obtained elastic incoherent structure factor (EISF). The dashed line is the theoretical EISF considering the reorientation of the whole molecule around its molecular axis and the dotted line is that by considering the reorientation of the butyloxy and octyl chain group around its chain axis in addition to the reorientation of the whole molecule. The theoretical EISFs have been calculated using the same methodology as used in the case of 5O.6 above. It is clear from Fig. 12 that rotations along the chain axis plus rotation about the molecular body axis can not explain the data in smectic *A* and nematic phases. Introducing a certain amount of fluctuation to the long molecular axis as is done in the case of 5O.6 while explaining its smectic *A* and nematic phases, one can explain the EISF at S_A and nematic phases of 4O.8 also. In Fig. 12, the solid lines are the theoretical EISF calculated with $\Delta\alpha=14°$ and 29° using the method described for 5O.6. These values of $\Delta\alpha$ correspond to the order parameter $S_1=0.97$ and 0.87 for smectic *A* and nematic phases. The variation of the HWHM of the quasielastic component with *Q* is shown in Fig. 13 for S_A and *N* phases.

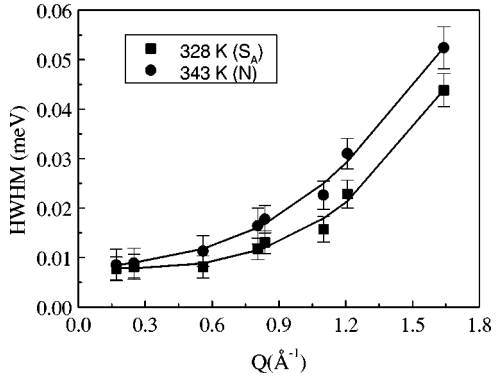

FIG. 13. Variation of the HWHM of the quasielastic component with *Q* in S_A and nematic phases in 4O.8. Solid lines are guides to the eye.

Body axis fluctuations along with the rotation of the whole molecule around its long axis are reported in a TBBA liquid crystal [12,13] and also in liquid crystal phases in the octaphenylcyclotetrasiloxane (OPCTS) molecule [24]. It may be noted that we have assumed that the chains are rigid and flexibility of the chains is not considered because that could lead to a complicated scenario.

IV. CONCLUSIONS

A quasielastic neutron scattering study in two members of the $n\mathrm{O}.m$ series (5O.6 and 4O.8) of liquid crystal showed the presence of simultaneous reorientational motions of the end chain around the chain axis and the whole molecule around the molecular axis in smectic S_G,S_B,S_C phases. However, in smectic *A* (the most disordered smectic phase) and nematic phases additional body axis fluctuation sets in. While the QENS data for 5O.6 at its smectic *A* and nematic phases were explained with an average amplitude of fluctuations, 15° and 25°, respectively, which is equivalent to an order parameter S_1 equal to ~0.97 and 0.91, respectively. The same in the smectic *A* and nematic phases of 4O.8 are found to be 14° and 29°, which is equivalent to an order parameter S_1 equal to ~0.97 and 0.87, respectively. The fluctuation is in addition to the simultaneous reorientation of the whole molecule around the body axis and the reorientations of the end chains around the chain axis. The higher amplitude of fluctuation in 4O.8 compared to 5O.6 in the nematic phase is perhaps due to the higher imbalance in the structure and also as it exists at higher temperature (335/343 K). These types of body axis fluctuations are reported in liquid crystals TBBA and OPCTS [12,24]. The present study shows that it is possible to successfully separate the dynamical contributions from the different parts of the molecule from the same experiment without using deuterated samples. Our results are consistent within themselves and with the earlier reports.

[1] J. B. Flannery and W. Hans, J. Phys. Chem. **74**, 3611 (1970).
[2] G. W. Smith and Z. G. Gardlund, J. Chem. Phys. **59**, 3214 (1973).
[3] V. Graf, F. Noack, and M. Stohrer, Z. Naturforsch. A **32A**, 61 (1977).
[4] J. R. Owers-Bradley, I. D. Clader, J. B. Ketterson, and W. P. Helperin, Mol. Cryst. Liq. Cryst. **76**, 175 (1981).
[5] A. C. Rabeiro, Mol. Cryst. Liq. Cryst. **151**, 261 (1987).
[6] G. Ravindranath, K. Venu, and V. S. S. Sastry, Phase Transitions **12**, 129 (1988).
[7] G. Ravindranath, K. Venu, and V. S. S. Sastry, Z. Phys. B: Condens. Matter **78**, 234 (1990).
[8] G. Ravindranath, K. Venu, and V. S. S. Sastry, Chem. Phys. **140**, 299 (1990).
[9] K. Venu, G. Ravindranath, and V. S. S. Sastry, Liq. Cryst. **8**, 81 (1990).
[10] S. Mitra, R. Mukhopadhyay, and K. Venu, Chem. Phys. **261**, 149 (2000).
[11] F. Volino, A. J. Dianoux, R. E. Lechner, and H. Hervet, J. Phys. Colloq. **36**, C1-83 (1975).
[12] F. Volino, A. J. Dianoux, and H. Hervet, J. Phys. Colloq. **37**, C3-55 (1976).
[13] F. Volino, A. J. Dianoux, and H. Hervet, Mol. Cryst. Liq. Cryst. **38**, 125 (1977).
[14] H. Hervet, F. Volino, A. J. Dianoux, and R. E. Lechner, J. Phys. (France) Lett. **35**, L151 (1974).
[15] H. Hervet, F. Volino, A. J. Dianoux, and R. E. Lechner, Phys. Rev. Lett. **34**, 451 (1975).
[16] H. Hervet, A. J. Dianoux, F. Volino, and R. E. Lechner, J. Phys. (France) **37**, 587 (1976).
[17] J. Topler, B. Alefield, and T. Springer, Mol. Cryst. Liq. Cryst. **26**, 297 (1973).
[18] A. Wiegeleben, L. Richter, J. Deresch, and D. Demus, Mol. Cryst. Liq. Cryst. **59**, 329 (1980).
[19] K. Inoue, T. Kanaya, Y. Kiyanagi, S. Ikeda, K. Shibata, H. Iwasa, T. Kamiyama, N. Watanabe, and Y. Izumi, Nucl. Instrum. Methods Phys. Res. A **309**, 294 (1991).
[20] W. Press, *Single Particle Rotations in Molecular Crystals* (Springer-Verlag, Berlin, 1981).
[21] M. Bée, *Quasielastic Neutron Scattering* (Adam Hilger, Bristol, 1988).
[22] A. J. Dianoux, F. Volino, and H. Hervet, Mol. Phys. **30**, 1181 (1975).
[23] A. J. Leadbetter and M. A. Mazid, Mol. Cryst. Liq. Cryst. **65**, 265 (1981).
[24] M. Bée, A. J. Dianoux, and F. Volino, Mol. Phys. **54**, 221 (1984).